Scripta Materialia 150 (2018) 22–25

Contents lists available at ScienceDirect

Scripta Materialia

journal homepage: www.elsevier.com/locate/scriptamat

Regular article

Quantifying the synergetic strengthening in gradient material

Y.F. Wang [a], C.X. Huang [a,*], M.S. Wang [a], Y.S. Li [b,*], Y.T. Zhu [b,c]

[a] School of Aeronautics and Astronautics, Sichuan University, Chengdu 610065,China
[b] Nano and Heterogeneous Materials Center, School of Materials Science and Engineering, Nanjing University of Science and Technology, Nanjing 210094, China
[c] Department of Materials Science and Engineering, North Carolina State University, Raleigh, NC 27695, USA

ARTICLE INFO

Article history:
Received 12 January 2018
Received in revised form 9 February 2018
Accepted 23 February 2018
Available online xxxx

Keywords:
Gradient structure
Synergetic strengthening
Yield strength
Hardness

ABSTRACT

Synergetic strengthening in heterostructures is a new strengthening mechanism for metals. Here, a simple procedure based on the relationship between hardness increment and yield strength increment of corresponding homogeneous counterparts is proposed to quantitatively predict the synergetic strengthening effect in gradient-structured Cu-30 wt%Zn. The synergetic strengthening among incompatible domains accounts for >33% of yield strength. The gradient structure with higher volume fraction of gradient domains exhibits higher synergetic strengthening. These results provide a new method for evaluating synergetic strengthening in heterostructured materials.

To achieve superior combination of strength and ductility, material scientists have synthesized various heterostructured (HS) materials in the past decades, including the gradient structure [1–9], lamella/layered structure [10–13], multimodal structure [14,15], etc. [16]. The excellent mechanical responses of these HS materials indicate a promising way to fabricate advanced materials with high performance. However, in most of previous works the improvement of yield strength was just simply attributed to conventional Hall-Petch type strengthening mechanisms such as reduced grain size and high dislocation density in the harder domains [5,15,17]. The fundamental consideration of the strengthening effects of mechanical heterogeneity was largely neglected until an extra strength was revealed in gradient IF steel by Wu et al. [1].

During the yielding and plastic deformation stages of HS materials, forceful mutual constraint between heterogeneous domains can be activated to maintain strain continuity [2,11]. This synergetic mechanical behavior activates unusual dislocation activities and dominants the state, distribution and allocation of both internal stresses and plastic strain, resulting in an extraordinary strengthening mechanism which can significantly improve strength while retain acceptable ductility, i.e. synergetic strengthening [1,10,18,19]. For example, a macroscopic gradient distribution of bi-axial stress generated by elastic/plastic interaction between incompatible layers during yielding was revealed in gradient sample by finite element modeling, which contributed to prominent yield strength much higher than the sum of separate gradient layers [1]. Due to the partitioning of plastic strain and the development of back stress that is induced by the accumulation of geometrically necessary dislocations (GNDs), lamella-structured Ti exhibited a superior strength-ductility synergy that is not possible for homogenous counterpart [10]. In addition, the synergetic strengthening in laminate and gradient structures were also qualitatively investigated from the points of GNDs pile-up and evolution of back stress [3,4,12].

Generally, the synergetic strengthening in HS materials is estimated by the difference between the measured strength and the linear summation of properties of standalone components, i.e. the predictions from the volume fraction-based simple rule-of-mixture [1,11]. However, it is experimentally very difficult, if not impossible, to peel off all homogeneous components from integrated structure and measure their individual mechanical properties [2,4,15]. It is reasonable to believe that the extra strengthening observed by Wu et al. [1] in gradient IF steel was much smaller than the real synergetic strengthening of the whole sample, because they simply divided the gradient sample into a sandwich-like structure, i.e. a coarse-grained (CG) core and two gradient surface layers. To date, there is very lack of methods which can quantify the synergetic strengthening in HS materials effectively and simply.

Here, we propose a simple method to quantitatively calculate the synergetic strengthening in gradient structures. The relationship between structural gradient and synergetic strengthening effect is comparatively analyzed in two types of gradient structures with different volume fractions of gradient surface layer.

A brass (Cu-30 wt%Zn) plate with a thickness of 3.6 mm was annealed at 600 °C for 2 h and used as the baseline metal. In order to fabricate a thicker gradient layer, some samples were subjected to multiple-pass friction stir processing (FSP) firstly under flowing cold water, in which process an unthreaded pin in diameter of 3 mm and length of 1 mm was used [20]. Thereafter, a technique of rotationally

* Corresponding authors.
E-mail addresses: chxhuang@scu.edu.cn (C.X. Huang), liyusheng@njust.edu.cn (Y.S. Li).

https://doi.org/10.1016/j.scriptamat.2018.02.039
1359-6462/

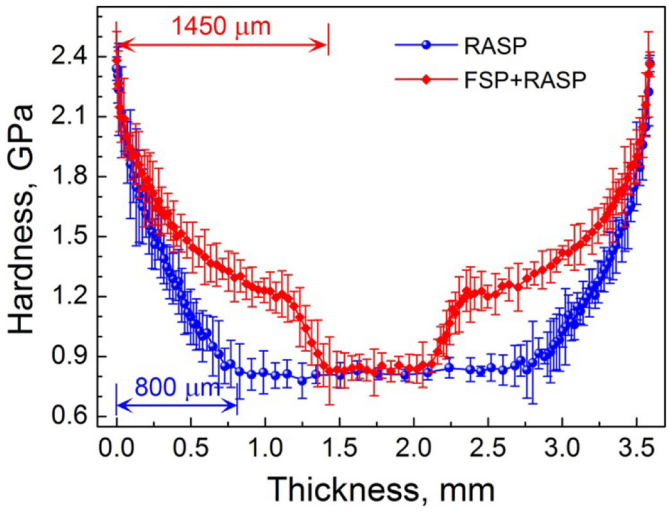

Fig. 1. Variation of the micro-hardness of G_{RASP} and $G_{FSP+RASP}$ samples along the thickness direction. Every data point was averaged from 4 indents.

accelerated shot peening (RASP) was conducted on both sides of all samples to produce the gradient surface layer [21]. The as-fabricated gradient materials were labeled as G_{RASP} and $G_{FSP+RASP}$, respectively. The gradient microstructures were characterized by transmission electron microscopy (TEM) and scanning electron microscopy (SEM) equipped with electron back-scattered diffraction (EBSD) detector. Dog-bone shaped tensile specimens with a gauge dimension of $20\times4\times3.6$ mm^3 were machined from the gradient plates. The Vickers micro-hardness was measured on the cross-section using a load of 25 g for 15 s.

Fig. 1 shows the micro-hardness profile across the whole thickness of gradient samples. The hardness reaches as high as 2.4 GPa in the topmost layers of both G_{RASP} and $G_{FSP+RASP}$ samples, which is ~3 times that of the CG core. Such a high mechanical incompatibility between surface and core layers is expected to produce great strain inhomogeneity during straining [2,11]. According to the hardness profiles, the thickness of gradient layer in the G_{RASP} and $G_{FSP+RASP}$ samples was measured as about 800 μm and 1450 μm, respectively. Note that the latter is much thicker than that achieved by standalone surface treatment techniques [21,22]. Here, the FSP process produces an ultrafine-grained (UFG) surface layer thicker than 1 mm and UFG-CG transition layer of ~450 μm [20]. After subsequent surface mechanical treatment by RASP to add a top nanocrystalline layer and enhance the mechanical gradient, stronger synergetic strengthening is expected than that of conventional gradient material with only a thin gradient surface layer.

The cross-sectional structure of the gradient surface layer of G_{RASP} material is shown in Fig. 2(a). A gradient variation of grain size from nano-grains in the topmost layer to equiaxed CG in matrix can be obviously observed. Fig. 2(b) shows a much thicker fine-grained layer with a thickness of ~1 mm in the $G_{FSP+RASP}$ sample. Fig. 2(c) is a typical bright-field TEM image and corresponding selected area electron diffraction pattern at the depth of ~25 μm below the treated surface in G_{RASP} material, showing well-developed nanostructures with random orientation. A similar microstructural observation was conducted in the top surface of the $G_{FSP+RASP}$ materials as well, and there was no obvious difference from that of the G_{RASP} sample. The $G_{FSP+RASP}$ sample still exhibits a UFG layer at the depth of ~950 μm that was produced by FSP, as seen in Fig. 2 (b) and (d). Fig. 2(e) is an EBSD map showing the UFG-CG transitional zone at the depth from 950 μm to 1450 μm in the $G_{FSP+RASP}$ sample.

Fig. 3 presents the typical tensile stress-strain curves of three different samples. The yield strengths (σ_y) of the G_{RASP} and $G_{FSP+RASP}$ samples are measured as 285 MPa and 422 MPa, respectively, which are about 3–4 times of pure CG sample (103 MPa). It is should be noted that the ductility of the G_{RASP} and $G_{FSP+RASP}$ samples are not superior compared with the gradient IF-steel and Cu [1,5]. This might be probably attributed to the high efficiency in grain refinement of Cu-30Zn during RASP due to the low stacking fault energy, which leads to low residual strain hardening capacity in the surface layers and thereby results in high incidence of crack nucleation from the nanostructured topmost layer and low efficiency in passivating crack propagation during tension.

There often exists a quantitative relationship between microhardness (Hv) and yield strength for homogeneous-structured material. For example, the widely used empirical formula [23]:

$$\sigma_y = Hv/3, \tag{1}$$

was constructed for materials not exhibiting work hardening. Although there is still much debate about the fitting parameters in the relationship between hardness and strength with regarding to different materials, the experimental data of either work-hardening or brittle materials usually can be well fitted by a linear equation [24]:

$$\sigma_y = k * Hv + y, \tag{2}$$

where k is the ratio that may deviate from 1/3, and y is the intercept

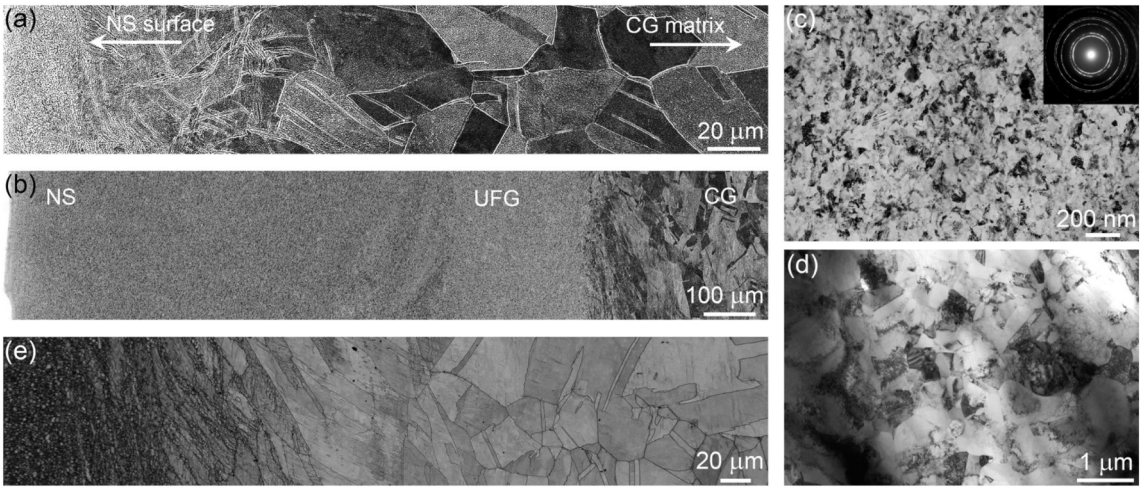

Fig. 2. Microstructure of the as-RASP (G_{RASP}) and as-FSP+RASP ($G_{FSP+RASP}$) processed gradient materials. (a) and (b) are SEM morphologies showing the cross-sectional gradient surface layer of the G_{RASP} and $G_{FSP+RASP}$ samples, respectively. (c) A typical TEM observation showing the nanostructure at the depth of ~25 μm in the G_{RASP} sample. (d) A TEM image showing the ultrafine grains at the depth of ~950 μm in the $G_{FSP+RASP}$ material. (e) An EBSD image showing the UFG-CG transitional microstructure in the $G_{FSP+RASP}$ material.